Convolutional Image Captioning

Jyoti Aneja*, Aditya Deshpande*, Alexander G. Schwing
University of Illinois at Urbana-Champaign
{janeja2, ardeshp2, aschwing}@illinois.edu

Abstract

Image captioning is an important task, applicable to virtual assistants, editing tools, image indexing, and support of the disabled. In recent years significant progress has been made in image captioning, using Recurrent Neural Networks powered by long-short-term-memory (LSTM) units. Despite mitigating the vanishing gradient problem, and despite their compelling ability to memorize dependencies, LSTM units are complex and inherently sequential across time. To address this issue, recent work has shown benefits of convolutional networks for machine translation and conditional image generation [9, 34, 35]. Inspired by their success, in this paper, we develop a convolutional image captioning technique. We demonstrate its efficacy on the challenging MSCOCO dataset and demonstrate performance on par with the LSTM baseline [16], while having a faster training time per number of parameters. We also perform a detailed analysis, providing compelling reasons in favor of convolutional language generation approaches.

1. Introduction

Image captioning, *i.e.*, describing the content observed in an image, has received a significant amount of attention in recent years. It is applicable in various scenarios, *e.g.*, recommendation in editing applications, usage in virtual assistants, for image indexing, and support of the disabled. With the availability of large datasets, deep neural network (DNN) based methods have been shown to achieve impressive results on image captioning tasks [16, 37]. These techniques are largely based on recurrent neural nets (RNNs), often powered by a Long-Short-Term-Memory (LSTM) [10] component.

LSTM nets have been considered as the de-facto standard for vision-language tasks of image captioning [5, 16, 37, 39, 38], visual question answering [3, 30, 28], question generation [14, 20], and visual dialog [7, 13], due to their compelling ability to memorize long-term dependencies through a memory cell. However, the complex addressing and overwriting mechanism combined with inherently sequential processing, and significant storage required due to back-propagation through time (BPTT), poses challenges during training. Also, in contrast to CNNs, that are non-sequential, LSTMs often require more careful engineering, when considering a novel task. Previously, CNNs have not matched up to the LSTM performance on vision-language tasks. Inspired by the recent successes of convolutional architectures on other sequence-to-sequence tasks – conditional image generation [34], machine translation [9, 35] – we study convolutional architectures for the vision-language task of image captioning. To the best of our knowledge, ours is the first convolutional network for image captioning that compares favorably to LSTM-based methods.

Our key contributions are: **a)** A convolutional (CNN-based) image captioning method that shows comparable performance to an LSTM based method [16] (Section 6.2, Table 1 and Table 2); **b)** Improved performance with a CNN model that uses attention mechanism to leverage spatial image features. With attention, we outperform the attention baseline [39] and qualitatively demonstrate that our method finds salient objects in the image. (Figure 5, Table 2); **c)** We analyze the characteristics of CNN and LSTM nets and provide useful insights such as – CNNs produce more entropy (useful for diverse predictions), better classification accuracy, and do not suffer from vanishing gradients (Section 6 and Figure 6, 7 and 8). We evaluate our architecture on the challenging MSCOCO [18] dataset, and compare it to an LSTM [16] and an LSTM+Attention baseline [39].

The paper is organized as follows: Section 2 gives our notation, Section 3 reviews the RNN based approach, Section 4 describes our convolutional method, Section 5 gives the details of CNN architecture, Section 6 contains results and Section 7 discusses related work.

2. Problem Setup and Notation

For image captioning, we are given an input image I and we want to generate a sequence of words $y = (y_1, \ldots, y_N)$. The possible words y_i at time-step i are subsumed in a discrete set $\mathcal{Y}$ of options. Its size, $|\mathcal{Y}|$, easily reaches several

* Denotes equal contribution.

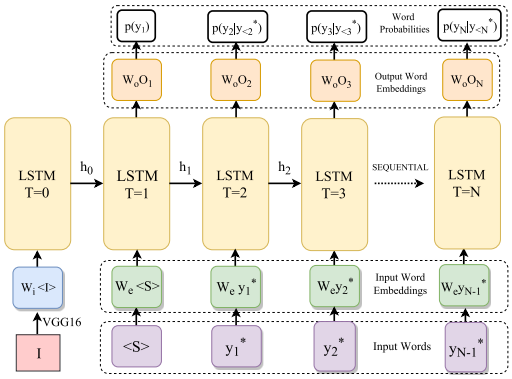

Figure 1: A sequential RNN powered by an LSTM cell. At each time step output is conditioned on the previously generated word, the image is fed at the start only.

thousands. $\mathcal{Y}$ contains special tokens that denote a start token (<S>), an end of sentence token (<E>), and an unknown token (<UNK>) which refers to all words not in $\mathcal{Y}$.

Given a training set $\mathcal{D} = \{(I, y^*)\}$ which contains pairs (I, y^*) of input image I and corresponding ground-truth caption $y^* = (y_1^*, \ldots, y_N^*)$, consisting of words $y_i^* \in \mathcal{Y}$, $i \in \{1, \ldots, N\}$, we maximize w.r.t. parameters w, a probabilistic model $p_w(y_1, \ldots, y_N | I)$.

A variety of probabilistic models have been considered (Section 7), from hidden Markov models [40] to recurrent neural networks.

3. RNN Approach

An illustration of a classical RNN architecture for image captioning is provided in Figure 1. It consists of three major components, all of which contain trainable parameters: the input word embeddings, the sequential LSTM units containing the memory cell, and the output word embeddings.

Inference. RNNs sequentially predict one word at a time, from y_1 up to y_N. At every time-step i, a conditional probability distribution $p_{i,w}(y_i | h_i, I)$, which depends on parameters w, is predicted (see top of Figure 1). For modeling $p_{i,w}(y_i | h_i, I)$, in the spirit of auto-regressive models, the dependence of word y_i on its ancestors $y_{<i}$ is implicitly captured by a hidden representation h_i (see arrows in Figure 1). Formally, the probability is computed via

$$p_{i,w}(y_i | h_i, I) = g_w(y_i, h_i, I), \tag{1}$$

where g_w can be any differentiable function/deep net. Note, image captioning techniques usually encode the image into the hidden representation h_0 (Figure 1).

Importantly, RNNs are described by a recurrence relation which governs computation of the hidden state h_i via

$$h_i = f_w(h_{i-1}, y_{i-1}, I). \tag{2}$$

Again, f_w can be any differentiable function. For image captioning, long-short-term-memory (LSTM) [10] nets and variants thereof based on gated recurrent units (GRU) [6], or forward-backward LSTM nets are used here.

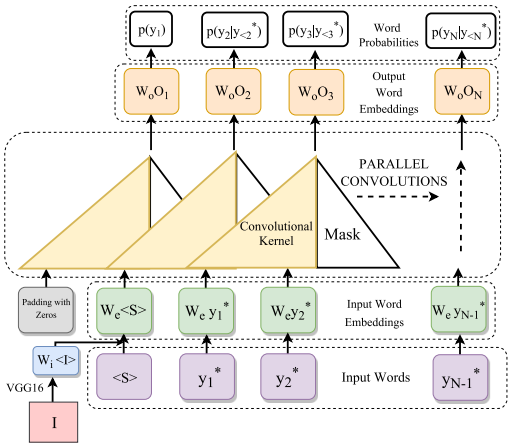

Figure 2: Our convolutional model for image captioning. We use a feed forward network with masked convolutions. Unlike RNNs, our model operates over all words in parallel.

Learning. Following classical supervised learning, it is common to find the parameters w of the word embeddings and the LSTM unit by minimizing the negative log-likelihood of the training data $\mathcal{D}$, *i.e.*, we optimize:

$$\min_w \sum_{\mathcal{D}} \sum_{i=1}^{N} -\ln p_{i,w}(y_i^* | h_i, I). \tag{3}$$

To compute the gradient of the objective given in Eq. (3), we use back-propagation through time (BPTT). BPTT is necessary due to the recurrence relationship encoded in f_w (Eq. (2)). Note, the gradients of the function f_w at time i depend on the gradients obtained in successive time-steps.

To avoid more complicated gradient flows through the recurrence relationship, during training, it is common to use

$$h_i = f_w(h_{i-1}, y_{i-1}^*, I), \tag{4}$$

rather than the form provided in Eq. (2). *I.e.*, during training, when computing the latent representation h_i, we use the ground-truth symbol y_{i-1}^* rather than the prediction y_{i-1}. This is termed as teacher forcing.

Although highly successful, RNN-based techniques suffer from some drawbacks. First, the training process is inherently sequential for a particular image-caption pair. This results from unrolling the recurrent relation in time. Hence, the output at time-step i has a true dependency on the output at $i-1$. Secondly, as we will show in our results for image captioning, RNNs tend to produce lower classification accuracy (Figure 6), and, despite LSTM units, they still suffer to some degree from vanishing gradients (Figure 8).

Next, we describe an alternative convolutional approach to image captioning which attempts to overcome some of these challenges.

4. Convolutional Approach

Our model is based on the convolutional machine translation model used in [9]. Figure 2 provides an overview of

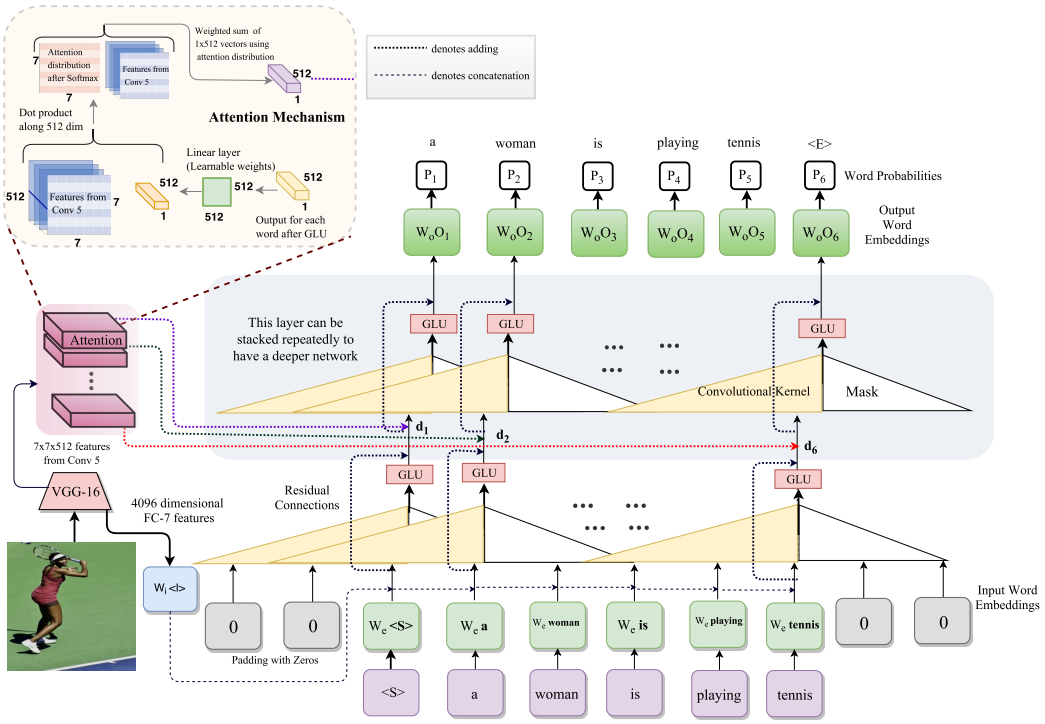

Figure 3: Our convolutional architecture for image captioning. It has four components: (i) Input embedding layer, (ii) Image embedding, (iii) Convolutional module and (iv) Output embedding layer. Details of each component are in Section 5.

our feed-forward convolutional (or CNN-based) approach for image captioning. As the figure illustrates, our technique contains three main components similar to the RNN technique. The first and the last components are input/output word embeddings respectively, in both cases. However, while the middle component contains LSTM or GRU units in the RNN case, masked convolutions are employed in our CNN-based approach. This component, unlike the RNN, is feed-forward without any recurrent function. We briefly review inference and learning of our model.

Inference. In contrast to the RNN formulation, where the probabilistic model is unrolled in time via the recurrence relation given in Eq. (2), we use a simple feed-forward deep net, f_w, for modeling $p_{i,w}(y_i|I)$. Prediction of a word y_i relies on past words $y_{<i}$ or their representations:

$$p_{i,w}(y_i|y_{<i}, I) = f_w(y_i, y_{<i}, I). \tag{5}$$

To disallow convolution operations from using information of future word tokens, we use masked convolutional layers that operate only on 'past' data [9, 34].

Inference can now be performed sequentially, one word at a time. Hence, inference begins with the start token <S> and employs a feed-forward pass to generate $p_{1,w}(y_1|\emptyset, I)$. Afterwards, $y_1 \sim p_{1,w}(y_1|\emptyset, I)$ is sampled. Note that it is possible to retrieve the maximizing argument or to perform beam search. After sampling, y_1 is fed back into the feed-forward network to generate subsequent words y_2, *etc*. Inference continues until the end token is predicted, or until we reach a fixed upper bound of N steps.

Learning. Similar to RNN training, we use ground-truth $y^*_{<i}$ for past words, instead of using the predicted word. For prediction of word probability $p_{i,w}(y_i|y^*_{<i}, I)$, the considered feed-forward network is $f_w(y_i, y^*_{<i}, I)$ and we optimize for parameters w using a likelihood similar to Eq. (3).

Since there are no recurrent connections and all ground-truth words are available at any given time-step i, our CNN based model can be trained in parallel for all words. In Section 5, we describe our convolutional architecture in detail.

5. Architecture

In Figure 3, we show a training iteration of our convolutional architecture with input (ground-truth) words $\{y^*_1, \ldots, y^*_5\}$ = { a, woman, is, playing, tennis }. Additionally, we add the start token <S> at the beginning, and also the end of sentence token <E>.

These words are processed as follows: (1) they pass through an input embedding layer; (2) they are combined with the image embedding; (3) they are processed by the CNN module; and (4) the output embedding (or classification) layer produces output probability distributions (see $\{p_1, \ldots, p_6\}$ at top of Figure 3). Each of the four aforementioned steps is discussed below.

Input Embedding. For consistency with the RNN/LSTM baseline, we train (from scratch) an embedding layer over one-hot encoded input words. We use $|\mathcal{Y}| = 9221$ and we embed the input words to 512-dimensional vectors, following the baseline. This embedding is concatenated to the image embedding (discussed next) and provided as input to the

Method	MSCOCO Val Set								MSCOCO Test Set							
	B1	B2	B3	B4	M	R	C	S	B1	B2	B3	B4	M	R	C	S
Baselines:																
LSTM [16]	**.710**	.535	.389	.281	**.244**	**.521**	**.899**	.169	**.713**	**.541**	**.404**	**.303**	**.247**	**.525**	**.912**	.172
LSTM + Attn (Soft) [39]	-	-	-	-	-	-	-	-	.707	.492	.344	.243	.239	-	-	-
LSTM + Attn (Hard) [39]	-	-	-	-	-	-	-	-	.718	.504	.357	.250	.230	-	-	-
Our CNN:																
CNN	.693	.518	.374	.268	.238	.511	.855	.167	.695	.521	.380	.276	.241	.514	.881	.171
CNN + Weight Norm.	.702	.528	.384	.279	.242	.517	.881	.169	.699	.525	.382	.276	.241	.516	.878	.170
CNN +WN +Dropout	.707	.532	.386	.278	.242	.517	.883	.171	.704	.532	.389	.283	.243	.520	.904	.173
CNN +WN +Dropout +Residual	.706	.532	.389	**.284**	**.244**	.519	**.899**	**.173**	.704	.532	.389	.284	.244	.520	.906	**.175**
CNN +WN +Drop. +Res. +Attn	**.710**	**.537**	**.391**	.281	.241	.519	.890	.171	.711	.538	.394	.287	.244	.522	**.912**	**.175**

Table 1: Comparison of different methods on standard evaluation metrics: BLEU-1 (B1), BLEU-2 (B2), BLEU-3 (B3), BLEU-4 (B4), METEOR (M), ROUGE (R), CIDEr (C) and SPICE (S). Our CNN with attention (attn) achieves comparable performance (equal CIDEr scores on MSCOCO test set) to [16] and outperforms LSTM+Attention baseline of [39]. We start with a CNN comprising masked convolutions and fully connected layers only. Then, we add weight normalization, dropout, residual connections and attention incrementally and show that performance improves with every addition. Here, for CNN and [16] we use the model that obtains the best CIDEr scores on val-set (over 30 epochs) and report its scores for the test set. For [39], we report all the available metrics for soft/hard attention from their paper (missing numbers are marked by -).

feed-forward CNN module.

Image Embedding. Image features for image I are obtained from the fc7 layer of the VGG16 network [31]. The VGG16 is pre-trained on the ImageNet dataset [27]. We apply dropout, ReLU on the fc7 and use a linear layer to obtain a 512-dimensional embedding. This is consistent with the image features used in the baseline LSTM method [16].

CNN Module. The CNN module operates on the combined input and image embedding vector. It performs three layers of masked convolutions. Consistent with [9, 34], we use gated linear unit (or GLU) activations for our conv layers. However, we did not observe a significant change in performance when using the standard ReLU activation. The feature dimension after convolution layer and GLU is 512. We add weight normalization, residual connections and dropout in these layers as they help improve performance (Table 1). Our masked convolutions have a receptive field of 5 words in the past. We set N (steps or max-sentence length) to 15 for both CNN/RNN. The output of the CNN module after three layers is a 512-dimensional vector for each word.

Classification Layer. We use a linear layer to encode the 512-dimensional vectors obtained from the CNN module into a 256-dimensional representation per word. Then, we upsample this vector to a $|\mathcal{Y}|$-dimensional activation via a fully connected layer, and pass it through a softmax to obtain the output word probabilities $p_{i,w}(y_i|y_{<i}, I)$.

Training. We use a cross-entropy loss on the probabilities $p_{i,w}(y_i|y_{<i}, I)$ to train the CNN module and the embedding layers. Consistent with [16], we start to fine-tune VGG16 along with our network after 8 training epochs. We optimize with RMSProp using an initial learning rate of $5e^{-5}$ and decay it by multiplying with a factor of .1 every 15 epochs. All methods were trained for 30 epochs and we evaluate the metrics (in Section 6.2) on the validation set, after every epoch, to pick the best model for all methods.

5.1. Attention

In addition to the aforementioned CNN architecture, we also experiment with an attention mechanism, since attention benefited [9, 35]. We form an attended image vector of dimension 512 and add it to the word embedding at every layer (shown with red, green and blue arrows in Figure 3). We compute separate attention parameters and a separate attended vector for every word. To obtain this attended vector we predict 7×7 attention parameters, over the VGG16 max-pooled conv-5 features of dimensions $7 \times 7 \times 512$ [31]. We use attention on all three masked convolution layers in our CNN module. We continue to use the fc7 image embedding discussed above.

To discuss attention more formally, let d_j denote the embedding of word j in the conv module (*i.e.*, its activations after GLU shown in Figure 3), let W refer to a linear layer applied to d_j, let c_i denote a 512-dimensional spatial conv-5 feature at location i (in 7×7 feature map) and let a_{ij} indicate the attention parameters. With this notation at hand, the attention parameter a_{ij} is computed via $a_{ij} = \frac{\exp(W(d_j)^T c_i)}{\sum_i \exp(W(d_j)^T c_i)}$, and the attended image vector for word j is obtained from $\sum_i a_{ij} c_i$. Note that [39] uses the LSTM hidden state to compute the attention parameters. Instead, we compute attention parameters using the conv-layer activations. This form of attention mechanism was first proposed in [4].

Method	Beam Size=2								Beam Size=3								Beam Size=4							
	B1	B2	B3	B4	M	R	C	S	B1	B2	B3	B4	M	R	C	S	B1	B2	B3	B4	M	R	C	S
LSTM [16]	.715	.545	.407	.304	.248	.526	.940	.178	.715	.544	.409	.310	.249	.528	.946	.178	.714	.543	.410	.311	**.250**	.529	.951	**.179**
CNN	.712	.541	.404	.303	.248	.527	.937	.178	.709	.538	.403	.303	.247	.525	.929	.176	.706	.533	.400	.302	.247	.522	.925	.175
CNN+Attn	.718	.549	.411	.306	.248	.528	.942	.177	**.722**	**.553**	**.418**	**.316**	**.250**	**.531**	**.952**	**.179**	.718	.550	.415	.314	.249	.528	.951	.179

Table 2: Comparison of different methods (metrics same as Table 1) with beam search on the output word probabilities. Our results show that with beam size$=3$ our CNN outperforms LSTM [16] on all metrics. Note, compared to Table 1, the performance improves with beam search. We use the MS COCO test split for this experiment. For beam search, we pick one caption with maximum log probability (sum of log probability of words) from the top-k beams and report the above metrics for it. Beam $= 1$ is same as the test set results reported in Table 1.

	c5 (Beam = 1)							c40 (Beam = 1)						
	B1	B2	B3	B4	M	R	C	B1	B2	B3	B4	M	R	C
LSTM	.704	.528	.384	.278	**.241**	**.517**	**.876**	.880	.778	.656	.537	**.321**	.655	**.898**
CNN+Attn	**.708**	**.534**	**.389**	**.280**	**.241**	**.517**	.872	**.883**	**.786**	**.667**	**.545**	**.321**	**.657**	.893
	c5 (Beam = 3)							c40 (Beam = 3)						
	B1	B2	B3	B4	M	R	C	B1	B2	B3	B4	M	R	C
LSTM	.710	.537	.399	.299	**.246**	.523	.904	.889	.794	.681	.570	**.334**	.671	.912
CNN+Attn	**.715**	**.545**	**.408**	**.304**	**.246**	**.525**	**.910**	**.896**	**.805**	**.694**	**.582**	.333	**.673**	**.914**

Table 3: Above, we show that CNN outperforms LSTM on BLEU metrics and gives comparable scores to LSTM on other metrics for test split on MSCOCO evaluation server. Note, this hidden test split of $40,775$ images on the evaluation server is different from the 5000 images test split used in Tables 1 and 2. We compare our CNN+Attn method to the LSTM baseline (metrics same as Table 1). The $c5, c40$ scores above are computed with $5, 40$ reference captions per test image respectively. We show comparison results for beam size 1 and beam size 3 for both the methods.

6. Results and Analysis

In this section, we demonstrate the following results:

- Our convolutional (or CNN) approach performs on par with LSTM (or RNN) based approaches on image captioning metrics (Table 1). Our performance improves with beam search (Table 2).
- Adding attention to our CNN gives improvements on metrics and we outperform the LSTM+Attn baseline [39] (Table 1). Figure 5 shows that with attention we identify salient objects for the given image.
- We analyze the CNN and RNN approaches and show that CNN produces (1) more entropy in the output probability distribution, (2) gives better word prediction accuracy (Figure 6), and (3) does not suffer as much from vanishing gradients (Figure 8).
- In Table 4, we show that a CNN with $1.5\times$ more parameters can be trained in comparable time. This is because we avoid the sequential processing of RNNs.

The details of our experimental setup and these results are discussed below. The PyTorch implementation of our convolutional image captioning is available on github.[1]

[1] https://github.com/aditya12agd5/convcap

6.1. Dataset and Baselines

We conducted experiments on the **MS COCO** dataset [18]. Our train/val/test splits follow [16, 39]. We use 113287 training images, 5000 images for validation, and 5000 for testing. Henceforth, we will refer to our approach as CNN, and our approach with the attention (Section 5.1) as CNN+Attn. We use the following naming convention for our baselines: [16] is denoted by LSTM and [39] is referred to as LSTM+Attn.

6.2. Comparison on Image Captioning Metrics

We consider multiple conventional evaluation metrics, BLEU-1, BLEU-2, BLEU-3, BLEU-4 [23], METEOR [8], ROUGE [17], CIDEr [36] and SPICE [1]. See Table 1 for the performance on all these metrics for our val/test splits. Note that we obtain comparable CIDEr scores and better SPICE scores than LSTM on test set with our CNN+Attn method. Our BLEU, METEOR, ROUGE scores are less than the LSTM ones, but the margin is very small. Our CNN+Attn method outperforms the LSTM+Attn baseline on the test set for all metrics reported in [39]. For Table 1, we form the caption by choosing the word with maximum probability at each step. The metrics are reported for this one caption formed by choosing the maximum probability word at every step.

Instead of sampling the maximum probability words, we also perform beam search with different beam sizes. We

LSTM: a man and a woman in a suit and tie
CNN: a black and white photo of a man and woman in a suit
GT: A man sitting next to a woman while wearing a suit.

LSTM: a cat is laying down on a bed
CNN: a polar bear is drinking water from a white bowl
GT: A white polar bear laying on top of a pool of water

LSTM: a bear is standing on a rock in a zoo
CNN: two bears are walking on a rock in the zoo
GT: two bears touching noses standing on rocks

LSTM: a box of donuts with a variety of toppings
CNN: a box of doughnuts with sprinkles and a sign
GT:A bunch of doughnuts with sprinkles on them

LSTM: a dog and a dog in a field
CNN: two cows are standing in a field of grass
GT: A dog and a horse standing near each other

Figure 4: Captions generated by our CNN are compared to the LSTM and ground-truth caption. In the examples above our CNN can describe things like black and white photo, polar bear/white bowl, number of bears, sign in the donut image which LSTM fails to do. The last image (rightmost) shows a failure case for CNN. Typically we observe that CNN and LSTM captions are of similar quality. We use our CNN+Attn method (Section 5.1) and the MSCOCO test split for these results.

perform beam search for both LSTM and our CNN methods. With beam search, we pick the maximum probability caption (sum of log word probability in the beam). The results reported in Table 2 demonstrate that with beam size of 3 we achieve better BLEU, ROUGE, CIDEr scores than LSTM and equal METEOR and SPICE scores.

In Table 3, we show the results obtained on the MSCOCO evaluation server. These results are computed over a test set of $40,775$ images for which ground-truth is not publicly available. We demonstrate that our method does better on all BLEU metrics, especially with beam size 3, we perform better than the LSTM based method.

Comparison to recent state-of-the-art. For better performance on the MSCOCO leader board we use ResNet features instead of VGG-16. Table 5 shows ResNet boosts our performance on the MSCOCO split (cf. Table 1) and we compare it to more recent methods [2] and [41]. We are almost as good as [41]. If we had access to their pre-trained attribute network, we may outperform it. [2] uses a sophisticated attention mechanism, which can be incorporated into our architecture as part of future work.

6.3. Qualitative Comparison

See Figure 4 for a qualitative comparison of captions generated by CNN and LSTM. In Figure 5, we overlay the attention parameters on the image for each word prediction. Note that our attention parameters are 7×7 as described in Section 5.1 and therefore the image is divided in a 7×7 grid. These results show that our attention focuses on salient objects such as man, broccoli, ocean, bench, *etc*., when predicting these respective words. Our results also show that the attention is uniform when predicting words such as a, of, on, *etc*., which are unrelated to the image content.

6.4. Analysis of CNN and RNN

In Table 4 we report the number of trainable parameters and the training time per epoch. CNNs with $\sim 1.5\times$ parameters can be trained in comparable time.

Table 1, 2 and 3 show that we obtain comparable performance from both CNN and RNN/LSTM-based methods. Encouraged by this result, we analyze the characteristics of these two methods. For fair comparison, we use our CNN without attention, since the RNN method does not use spatial image features. First, we compare the negative log-likelihoods (or cross-entropy loss) on a subset of train and the entire val set (see Figure 6 (a)). We find that the loss is higher for CNN than RNN. This is because CNNs are being penalized for producing less-peaky word probability distributions. To evaluate this further, we plot the entropy of the output probability distribution (Figure 6 (b)) and the classification accuracy, *i.e*., the number of times the maximum probability word is the ground truth (Figure 6 (c)). These plots show that RNNs are good at producing low entropy and therefore peaky word probability distributions at the output, while CNNs produce less peaky distributions (and high entropy). Less peaky distributions are not necessarily bad, particularly for a problem like image captioning, where multiple word predictions are possible. Despite, less peaky distributions, Figure 6 (c) shows that the maximum probability word is correct more often on the train set and it is within approx. 1% accuracy on the val set. Note, cross-entropy loss is a proxy for the classification accuracy and we show that CNNs have higher cross entropy loss, but their classification accuracy is good. Less peaky posterior distributions provided by a CNN may be indicative of CNNs being more capable of predicting diverse captions.

Diversity. In Figure 7, we plot the unique words and 2/4-grams predicted at every word position or time-step. The plot is for word positions 1 to 13. This plot shows that for the CNN we have higher unique words for more word positions and consistently higher 2/4-grams than LSTM. This supports our analysis that CNNs have less peaky (or one-hot) posteriors and therefore can produce more diversity. For these diversity experiments, we perform a beam search with beam size 10 and use all the top 10 beams.

Vanishing Gradient. Since RNNs/LSTMs are known

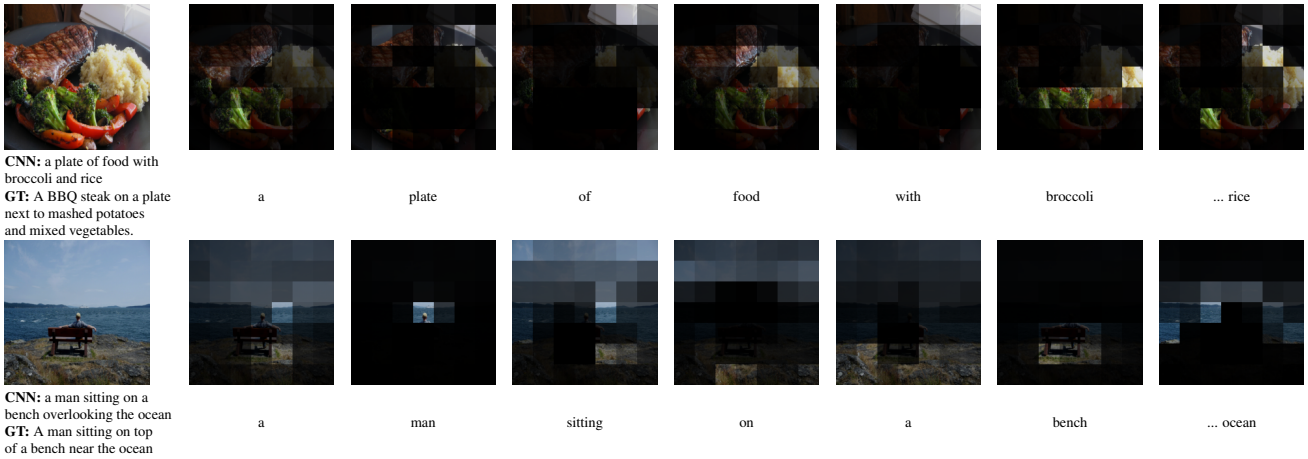

Figure 5: Attention parameters are overlayed on the image. These results show that we focus on salient regions as broccoli, bench when predicting these words and that the attention is uniform when predicting words such as a, of and on.

Method	# Parameters	Train time per epoch
LSTM [16]	13M	1529s
Our CNN	19M	1585s
Our CNN+Attn	20M	1620s

Table 4: We train a CNN faster per parameter than the LSTM. This is because CNN is not sequential like the LSTM. We use PyTorch implementation of [16] and our CNN-based method, and the timings are obtained on Nvidia Titan X GPU.

Method	B1	B2	B3	B4	M	R	C
Our Resnet-101	.72	.549	.403	.293	.248	.527	.945
Our Resnet-152	**.725**	**.555**	**.41**	**.299**	**.251**	**.532**	**.972**
LSTM Resnet-152	.724	.552	.405	.294	**.251**	**.532**	.961
[41] Resnet-152	.731	.564	.426	.321	.252	.537	.984
[2] Resnet-101	.772	-	-	.362	.27	.564	1.13

Table 5: Comparison to recent state-of-the-art with Resnet.

to suffer from vanishing gradient problems, in Figure 8, we plot the gradient norm at the output embedding/classification layer and the gradient norm at the input embedding layer. The values are averaged over 1 training epoch. These plots show that the gradients in RNN/LSTM diminishes more than the ones in CNNs. Hence RNN/LSTM nets are more likely to suffer from vanishing gradients, which stalls learning. If learning is stalled, for larger datasets than the ones we currently use for image captioning, the performance of RNN and CNN may differ significantly.

7. Related Work

Describing the content of an observed image is related to a large variety of tasks. Object detection [25, 26, 42] and semantic segmentation [21, 29, 12] can be used to obtain a list of objects. Detection of co-occurrence patterns and relationships between objects can help to form sentences. Generating sentences by taking advantage of surrogate tasks is then a multi-step approach which is beneficial for interpretability but lacks a joint objective that can be trained end-to-end.

Early techniques formulate image captioning as a retrieval problem and find the best fitting description from a pool of possible captions [11, 15, 22, 32]. Those techniques are built upon the idea that the fitness between available textual descriptions and images can be learned. While this permits end-to-end training, matching image descriptors to a sufficiently large pool of captions is computationally expensive. In addition, constructing a database of captions that is sufficient for describing a reasonably large fraction of images seems prohibitive.

To address this issue, recurrent neural nets (RNNs) or probabilistic models like Markov chains, which decompose the space of a caption into a product space of individual words are compelling. The success of RNNs for image captioning is based on a key component, *i.e.*, the Long-Short-Term-Memory (LSTM) [10] or recent alternatives like the gated recurrent unit (GRU) [6]. These components capture long-term dependencies by adding a memory cell, and they address the vanishing or exploding gradient issue of classical RNNs to some degree.

Based on this success, [19] train a vision (or image) CNN and a language RNN that shares a joint embedding layer. [37] jointly train a vision (or image) CNN with a language RNN to generate sentences, [39] extends [37] with additional attention parameters and learns to identify salient objects for caption generation. [16] use a bi-directional RNN along with a structured loss function in a shared vision-language space. [41] use an additional network trained on coco-attributes, and [2, 28] develop an attention mechanism for captioning. These recurrent neural nets have found widespread use for captioning because they

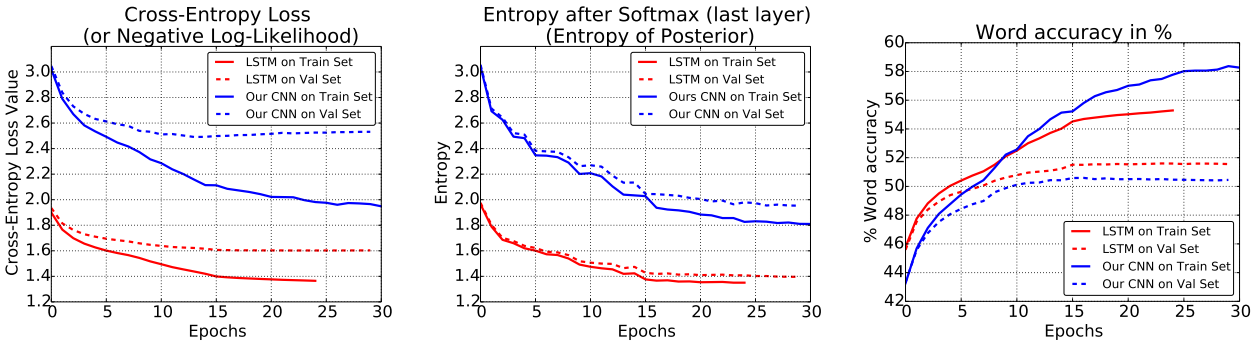

(a) CNN gives higher cross-entropy loss on train/val set of MSCOCO compared to LSTM. But, as we show in (c), CNN obtains better % word accuracy than LSTM. Therefore, it assigns max. probability to correct word. The CNN loss is high because its output probability distributions have more entropy than LSTM.

(b) The entropy of the softmax layer (or posterior probability distribution) of our CNN is higher than the LSTM. For ambiguous problems such as image captioning, it is desirable to have a less peaky (multi-modal) posterior (like ours) capable of producing multiple captions, rather than a peaky one (like LSTM).

(c) Even though the CNN training loss is higher than LSTM, its word prediction accuracy is better than LSTM on train set. On val set, the difference in accuracy between LSTM and CNN is small (only $\sim 1\%$).

Figure 6: In the figures above we plot (a) Cross-entropy loss, (b) Entropy of the softmax layer, (c) Word accuracy on train/val set. Blue line denotes our CNN and red denotes the LSTM based method [16]. Solid/dotted lines denote train/val set of MSCOCO respectively. For train set, we randomly sample 10k images and use the entire val set.

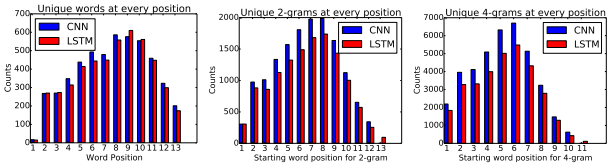

(a) Unique words (b) Unique 2-grams (c) Unique 4-grams

Figure 7: We perform beam search of beam size 10 with our best performing LSTM and CNN models. We use the top 10 beams to plot the unique words, 2/4-grams predicted for every word position. CNN (blue) produces higher unique words, 2/4-grams at more positions, and therefore more diversity, than LSTM (red).

have been shown to produce remarkably fitting descriptions.

Despite the fact that the above RNNs based on LSTM/GRU deliver remarkable results, *e.g.*, for image captioning, their training procedure is all but trivial. For instance, while the forward pass during training can be in parallel across samples, it is inherently sequential in time, limiting the parallelism. To address this issue, [34] proposed a PixelCNN architecture for conditional image generation that approximates an RNN. [9] and [35] demonstrate that convolutional architectures with attention achieve state-of-the-art performance on machine translation tasks. In spirit similar is our approach for image captioning, which is convolutional but addresses a different task.

8. Conclusion

We discussed a convolutional approach for image captioning and showed that it performs on par with existing LSTM techniques. We also analyzed the differences between RNN based learning and our method, and found

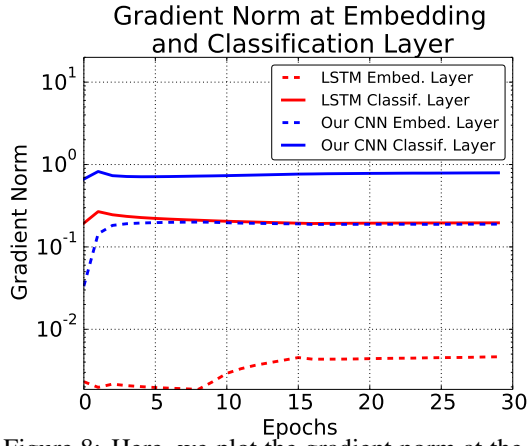

Figure 8: Here, we plot the gradient norm at the input embedding (dotted line) and output embedding/classification (solid line) layer. The gradient to the first layer of LSTM decays by a factor ~ 100 in contrast to our CNN, where it decays by a factor of ~ 10. There is prior evidence in literature that unlike CNNs, RNN/LSTMs suffer from vanishing gradients [24, 33].

gradients of lower magnitude as well as overly confident predictions to be existing LSTM network concerns.

Acknowledgments. We thank Arun Mallya for implementation of [16], Tanmay Gangwani for beam search code used for Figure 7 and we thank David Forsyth for insightful discussions and his comments. This material is based upon work supported in part by the National Science Foundation under Grant No. 1718221, NSF IIS-1421521 and by ONR MURI Award N00014-16-1-2007 and Samsung. We thank NVIDIA for the GPUs used for this work.

References

[1] P. Anderson, B. Fernando, M. Johnson, and S. Gould. Spice: Semantic propositional image caption evaluation. In *ECCV*, 2016. 5

[2] P. Anderson, X. He, C. Buehler, D. Teney, M. Johnson, S. Gould, and L. Zhang. Bottom-up and top-down attention for image captioning and visual question answering. *arXiv preprint arXiv:1707.07998*, 2017. 6, 7

[3] S. Antol, A. Agrawal, J. Lu, M. Mitchell, D. Batra, C. L. Zitnick, and D. Parikh. VQA: Visual Question Answering. In *International Conference on Computer Vision (ICCV)*, 2015. 1

[4] D. Bahdanau, K. Cho, and Y. Bengio. Neural machine translation by jointly learning to align and translate. *CoRR*, abs/1409.0473, 2014. 4

[5] X. Chen and C. L. Zitnick. Mind's eye: A recurrent visual representation for image caption generation. In *2015 IEEE Conference on Computer Vision and Pattern Recognition (CVPR)*, pages 2422–2431, June 2015. 1

[6] K. Cho, B. van Merriënboer, Ç. Gülçehre, D. Bahdanau, F. Bougares, H. Schwenk, and Y. Bengio. Learning phrase representations using rnn encoder–decoder for statistical machine translation. In *Proceedings of the 2014 Conference on Empirical Methods in Natural Language Processing (EMNLP)*, pages 1724–1734, Doha, Qatar, Oct. 2014. Association for Computational Linguistics. 2, 7

[7] A. Das, S. Kottur, K. Gupta, A. Singh, D. Yadav, J. M. F. Moura, D. Parikh, and D. Batra. Visual dialog. 2017. 1

[8] M. Denkowski and A. Lavie. Meteor universal: Language specific translation evaluation for any target language. In *Proceedings of the EACL 2014 Workshop on Statistical Machine Translation*, 2014. 5

[9] J. Gehring, M. Auli, D. Grangier, D. Yarats, and Y. N. Dauphin. Convolutional sequence to sequence learning. *CoRR*, abs/1705.03122, 2017. 1, 2, 3, 4, 8

[10] S. Hochreiter and J. Schmidhuber. Long short-term memory. *Neural Comput.*, 9(8):1735–1780, Nov. 1997. 1, 2, 7

[11] M. Hodosh, P. Young, and J. Hockenmaier. Framing image description as a ranking task: Data, models and evaluation metrics. *J. Artif. Int. Res.*, 47(1), May 2013. 7

[12] Y.-T. Hu, J.-B. Huang, and A. G. Schwing. MaskRNN: Instance Level Video Object Segmentation. In *Proc. NIPS*, 2017. 7

[13] U. Jain, S. Lazebnik, and A. G. Schwing. Two can play this Game: Visual Dialog with Discriminative Question Generation and Answering. In *Proc. CVPR*, 2018. 1

[14] U. Jain, Z. Zhang, and A. G. Schwing. Creativity: Generating diverse questions using variational autoencoders. In *Computer Vision and Pattern Recognition*, 2017. 1

[15] Y. Jia, M. Salzmann, and T. Darrell. Learning cross-modality similarity for multinomial data. In *Proceedings of the 2011 International Conference on Computer Vision*, ICCV '11, pages 2407–2414, Washington, DC, USA, 2011. IEEE Computer Society. 7

[16] A. Karpathy and L. Fei-Fei. Deep visual-semantic alignments for generating image descriptions. In *2015 IEEE Conference on Computer Vision and Pattern Recognition (CVPR)*, pages 3128–3137, June 2015. 1, 4, 5, 7, 8

[17] C.-Y. Lin. Rouge: a package for automatic evaluation of summaries. July 2004. 5

[18] T.-Y. Lin, M. Maire, S. Belongie, J. Hays, P. Perona, D. Ramanan, P. Dollár, and C. L. Zitnick. *Microsoft COCO: Common Objects in Context*, pages 740–755. Springer International Publishing, Cham, 2014. 1, 5

[19] J. Mao, W. Xu, Y. Yang, J. Wang, and A. L. Yuille. Deep captioning with multimodal recurrent neural networks (m-rnn). *CoRR*, abs/1412.6632, 2014. 7

[20] N. Mostafazadeh, I. Misra, J. Devlin, M. Mitchell, X. He, and L. Vanderwende. Generating natural questions about an image. In *ACL (1)*. The Association for Computer Linguistics, 2016. 1

[21] M. Mostajabi, P. Yadollahpour, and G. Shakhnarovich. Feedforward semantic segmentation with zoom-out features. In *2015 IEEE Conference on Computer Vision and Pattern Recognition (CVPR)*, pages 3376–3385, June 2015. 7

[22] V. Ordonez, G. Kulkarni, and T. L. Berg. Im2text: Describing images using 1 million captioned photographs. In *Proceedings of the 24th International Conference on Neural Information Processing Systems*, NIPS'11, pages 1143–1151, USA, 2011. Curran Associates Inc. 7

[23] K. Papineni, S. Roukos, T. Ward, and W.-J. Zhu. Bleu: A method for automatic evaluation of machine translation. In *Proceedings of the 40th Annual Meeting on Association for Computational Linguistics*, ACL '02, pages 311–318, Stroudsburg, PA, USA, 2002. Association for Computational Linguistics. 5

[24] R. Pascanu, T. Mikolov, and Y. Bengio. On the difficulty of training recurrent neural networks. In *Proceedings of the 30th International Conference on International Conference on Machine Learning - Volume 28*, ICML'13, pages III–1310–III–1318. JMLR.org, 2013. 8

[25] J. Redmon, S. K. Divvala, R. B. Girshick, and A. Farhadi. You only look once: Unified, real-time object detection. *CoRR*, abs/1506.02640, 2015. 7

[26] S. Ren, K. He, R. Girshick, and J. Sun. Faster r-cnn: Towards real-time object detection with region proposal networks. In *Proceedings of the 28th International Conference on Neural Information Processing Systems - Volume 1*, NIPS'15, pages 91–99, Cambridge, MA, USA, 2015. MIT Press. 7

[27] O. Russakovsky, J. Deng, H. Su, J. Krause, S. Satheesh, S. Ma, Z. Huang, A. Karpathy, A. Khosla, M. Bernstein, A. C. Berg, and L. Fei-Fei. Imagenet large scale visual recognition challenge. *International Journal of Computer Vision*, 115(3):211–252, Dec 2015. 4

[28] I. Schwartz, A. G. Schwing, and T. Hazan. High-Order Attention Models for Visual Question Answering. In *Proc. NIPS*, 2017. 1, 7

[29] E. Shelhamer, J. Long, and T. Darrell. Fully convolutional networks for semantic segmentation. *IEEE Trans. Pattern Anal. Mach. Intell.*, 39(4):640–651, Apr. 2017. 7

[30] K. J. Shih, S. Singh, and D. Hoiem. Where to look: Focus regions for visual question answering. In *Computer Vision and Pattern Recognition*, 2016. 1

[31] K. Simonyan and A. Zisserman. Very deep convolutional networks for large-scale image recognition. *CoRR*, abs/1409.1556, 2014. 4

[32] R. Socher, A. Karpathy, Q. Le, C. Manning, and A. Ng. Grounded compositional semantics for finding and describing images with sentences. *Transactions of the Association for Computational Linguistics*, 2:207–218, 2014. 7

[33] I. Sutskever, J. Martens, and G. Hinton. Generating text with recurrent neural networks. In L. Getoor and T. Scheffer, editors, *Proceedings of the 28th International Conference on Machine Learning (ICML-11)*, ICML '11, pages 1017–1024, New York, NY, USA, June 2011. ACM. 8

[34] A. van den Oord, N. Kalchbrenner, O. Vinyals, L. Espeholt, A. Graves, and K. Kavukcuoglu. Conditional image generation with pixelcnn decoders. In *NIPS*, 2016. 1, 3, 4, 8

[35] A. Vaswani, N. Shazeer, N. Parmar, J. Uszkoreit, L. Jones, A. N. Gomez, L. Kaiser, and I. Polosukhin. Attention is all you need. *CoRR*, abs/1706.03762, 2017. 1, 4, 8

[36] R. Vedantam, C. L. Zitnick, and D. Parikh. Cider: Consensus-based image description evaluation. In *CVPR*, pages 4566–4575. IEEE Computer Society, 2015. 5

[37] O. Vinyals, A. Toshev, S. Bengio, and D. Erhan. Show and tell: Lessons learned from the 2015 mscoco image captioning challenge. *IEEE Trans. Pattern Anal. Mach. Intell.*, 39(4):652–663, Apr. 2017. 1, 7

[38] L. Wang, A. G. Schwing, and S. Lazebnik. Diverse and Accurate Image Description Using a Variational Auto-Encoder with an Additive Gaussian Encoding Space. In *Proc. NIPS*, 2017. 1

[39] K. Xu, J. L. Ba, R. Kiros, K. Cho, A. Courville, R. Salakhutdinov, R. S. Zemel, and Y. Bengio. Show, attend and tell: Neural image caption generation with visual attention. In *Proceedings of the 32Nd International Conference on International Conference on Machine Learning - Volume 37*, ICML'15, pages 2048–2057. JMLR.org, 2015. 1, 4, 5, 7

[40] Y. Yang, C. L. Teo, H. Daumé, III, and Y. Aloimonos. Corpus-guided sentence generation of natural images. In *Proceedings of the Conference on Empirical Methods in Natural Language Processing*, EMNLP '11, pages 444–454, Stroudsburg, PA, USA, 2011. Association for Computational Linguistics. 2

[41] T. Yao, Y. Pan, Y. Li, Z. Qiu, and T. Mei. Boosting image captioning with attributes. In *IEEE International Conference on Computer Vision, ICCV 2017, Venice, Italy, October 22-29, 2017*, pages 4904–4912, 2017. 6, 7

[42] R. A. Yeh, J. Xiong, W.-M. Hwu, M. Do, and A. G. Schwing. Interpretable and Globally Optimal Prediction for Textual Grounding using Image Concepts. In *Proc. NIPS*, 2017. 7